Received: 20 April 2020 | Revised: 7 July 2020 | Accepted: 3 August 2020

DOI: 10.4218/etrij.2020-0169

ORIGINAL ARTICLE

ETRI Journal WILEY

Implementation of an in vitro exposure system for 28 GHz

Young Seung Lee[1] | **Philip Ayiku Dzagbletey**[2] | **Jae-Young Chung**[2] | **Sang Bong Jeon**[1] | **Ae-Kyoung Lee**[1] | **Nam Kim**[3] | **Seong Jong Song**[4] | **Hyung-Do Choi**[1]

[1]Radio and Satellite Research Division, Electronics and Telecommunications Research Institute, Daejeon, Rep. of Korea

[2]Department of Electrical and Information Engineering, Seoul National University of Science and Technology, Seoul, Rep. of Korea

[3]Department of Computer and Communication Engineering, Chungbuk National University, Cheongju, Rep. of Korea

[4]Management Planning Office, Dymstec, Seongnam, Rep. of Korea

Correspondence
Young Seung Lee, Radio and Satellite Research Division, Electronics and Telecommunications Research Institute, Daejeon, Rep. of Korea.
Email: lys009@etri.re.kr

Funding information
This work was supported by the ICT R&D program of MSIT/IITP. [2019-0-00102, A Study on Public Health and Safety in a Complex EMF Environment].

Abstract

The objective of this study was to implement an in vitro exposure system for 28 GHz to investigate the biological effects of fifth-generation (5G) communication. A signal source of 28 GHz for 5G millimeter-wave (MMW) deployment was developed, followed by a variable attenuator for antenna input power control. A power amplifier was also customized to ensure a maximum output power of 10 W for high-power 28-GHz exposure. A 3-dB uniformity over the 80 mm × 80 mm area that corresponds to four Petri dishes of three-dimensional cell cultures can be obtained using a customized choke-ring-type antenna. An infrared camera is employed for temperature regulation during exposure by adjusting the airflow cooling rate via real-time feedback to the incubator. The reported measurement results confirm that the input power control, uniformity, and temperature regulation for 28-GHz exposure were successfully accomplished, indicating the possibility of a wide application of the implemented in vitro exposure system in the fields of various MMW dose-response studies.

KEYWORDS

3D culture, exposure system, in vitro, integration, millimeter-wave, uniformity

1 | INTRODUCTION

Fifth-generation (5G) wireless communication technologies that support cellular networks have currently attracted considerable interest from various agencies and industries worldwide [1]. These 5G networks employ the frequency spectrum in the millimeter-wave (MMW) region such as the 28-GHz band [2] to fulfill the key 5G features and requirements defined in International Mobile Telecommunications-2020 (IMT-2020) [3], which are usually classified into three service categories: enhanced Mobile Broadband [4], massive Machine Type Communication [5], and Ultra-Reliable Low-Latency Communications [6]. In fact, the MMW frequency above 24 GHz is formally defined in the 3rd Generation Partnership Project (3GPP) specification as the new 5G operating spectrum band of "Frequency Range 2" [7]. Therefore, compliance assessment of 5G MMW mobile base stations [8] is now considered an important factor to ensure the public is safe from radiation exposure. The biological and health risks caused by electromagnetic field (EMF) exposure are assessed mainly based on in vivo and in vitro experiments. In particular, in vitro (cellular) studies conducted on cell cultures can provide the biological effects of exposures at relatively low cost and increase the reliability of in vivo (animal) studies that should be time intensive and consider ethical issues

[9]. EMF from 5G sources in the MMW range will only reach the superficial tissues owing to the small penetration depth of the radiation. The adverse health effects of these MMW-range EMFs will primarily be thermal with regard to the skin and eyes [10,11]. Various types of in vitro MMW exposure setups have been proposed experimentally [12,13] and numerically [14–16] to study the potential biological effects of MMW frequencies. However, little information regarding in vitro MMW setups based on the 5G spectrum has been published, as there are few natural sources of 5G MMW radiation because of the severe propagation losses associated with them [17].

This paper presents an implementation of an in vitro exposure system for 28 GHz, which is one of the main MMW frequency bands for 5G communications [2] in this context. Compared to other reported in vitro MMW exposure systems [12–16], little effort has been made to practically realize an in vitro experiment system for 5G MMW exposure. The entire system is based on field uniformity [18] to provide adequate exposure area for three-dimensional (3D) cell culture [19,20], which is more efficient in dealing with a shallow skin depth of approximately 1 mm at MMW frequencies [10]. A significant feature of the implemented system is its "all-in-one" characteristics, that is, every system component is incorporated into a single unit for a more accurate exposure experiment. A signal source with a 28-GHz frequency and a power amplifier are customized for high-power exposure up to a power density (PD) level of 500 W/m^2, which is several tens of times higher than the safety limit of 10 W/m^2 [21,22]. An infrared (IR) camera is also employed to record cell temperatures and maintain an optimal target temperature during exposures via real-time feedback to the incubator by adjusting the airflow cooling rate. Measurement results are also reported to verify the signal level control, uniformity, and temperature regulation.

2 | MATERIALS AND METHODS

2.1 | In vitro exposure system design

The system requirements of an in vitro 28-GHz exposure system based on simulations [18] are summarized in Table 1. A plane wave impedance of 377 Ω should be realized for each vertical distance d less than the distance of the far-field region to obtain good uniformity and reduce the chamber size. The 3-dB uniformity area (ie, the difference between the maximum and minimum values is 3 dB) of 80 mm × 80 mm stems from the four (2 × 2) 35 mm Petri dishes to minimize polarization effects. The center-to-center distance between the dishes is 39 mm. The system should support high-power MMW exposures of up to 500 W/m^2, which corresponds to a PD level that is 50 times higher than the permissible reference level for the public as per International Commission on Non-Ionizing Radiation Protection (ICNIRP) guidelines [21,22]. Hence, the input power level should also be adjustable for various dose-response data for this purpose. Temperature regulation and environmental control for stable long-term exposure are also required. All detailed optimizations and practical constructions, however, were carried out during the actual measurement and implementation of the system components.

TABLE 1 System requirements of an in vitro 28 GHz exposure system

Parameter	Specification
Wave impedance	377 Ω
Maximum MMW exposure	up to ~500 W/m^2
3-dB uniformity area	80 × 80 mm^2
Chamber size	40 × 40 × 40 cm^3
Additional req.	Temperature regulation etc.

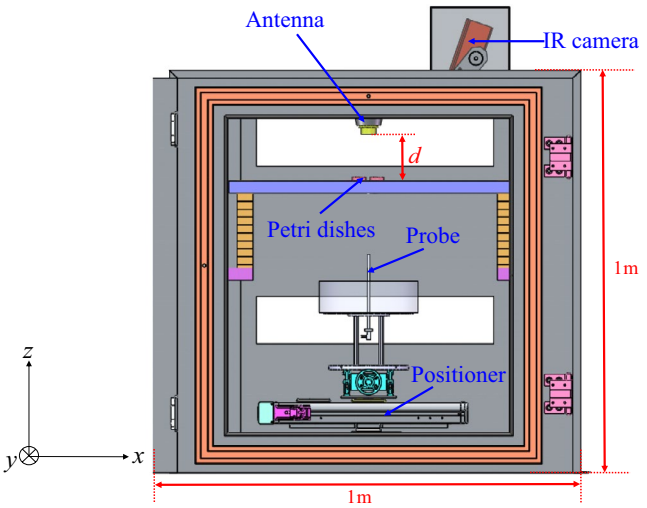

FIGURE 1 Schematic diagram of design for a 28 GHz exposure chamber

A schematic diagram of the proposed design for a 28-GHz exposure chamber is illustrated in Figure 1. The overall chamber size of 1000 mm × 1000 mm × 1000 mm is the result of additional space for the system components inside the chamber such as a waveguide probe, a positioner, and absorbers, as discussed below in detail.

2.2 | System implementation

2.2.1 | Exposure chamber

The chamber for in vitro 28-GHz experiments based on the proposed design is illustrated in Figure 2A. The MMW exposure chamber is embedded in an outer incubator to deliver a constant environment (temperature, relative humidity, and

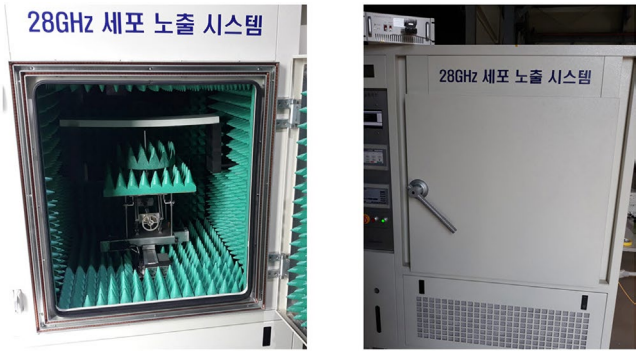

(A) (B)

FIGURE 2 Implemented in vitro 28 GHz exposure system: (A) exposure chamber embedded in the incubator and (B) front view of the overall system

TABLE 2 Simulated far-field characteristics of a choke-ring type antenna

	Principal planes		
Parameter	**E-plane**	**H-plane**	**45°-plane**
Gain (dB)	9.8	9.8	9.8
Beamwidth (°)	67.6	66.3	67.2
XPD	38.2	39.4	20.3

CO_2) for cell cultures, as shown in Figure 2B, constituting an integrated "all-in-one" in vitro MMW exposure system for successful experimentation in a controlled environment. The dimensions of the entire integrated system in Figure 2B are approximately 1600 mm × 1600 mm × 1958 mm.

A MMW 28-GHz continuous wave signal is generated by a signal source and then amplified by a power amplifier. Both the signal source and power amplifier are specifically customized for a 28-GHz in vitro exposure system. A signal source includes an HMC985ALP4KE variable attenuator (Analog Devices, Inc.) for signal power control. A power amplifier was fabricated using four gallium nitride high-electron-mobility transistors with a waveguide power combiner to improve the amplifier efficiency and achieve a maximum gain of 40 dB. The maximum output power of 10 W is achieved for a high PD of approximately 500 W/m^2 inside the exposure chamber. The antenna input power can also be controlled in steps of 0.1 W based on the measurement data of a variable attenuator voltage and amplifier output power, as discussed later.

A choke-ring-type antenna for 28-GHz uniformity was designed based on its broadbeam properties to obtain the wave impedance characteristics of a plane wave (377 Ω) in the field region shorter than the Rayleigh distance of $2D^2/\lambda$ (D is the largest dimension of the antenna), as shown in Table 1.

TABLE 3 Simulated wave impedance and uniformity characteristics of a choke-ring type antenna in terms of vertical distance d (see Figure 1)

Vertical distance d (mm)	Wave impedance (Ω)	Uniformity (dB)
100	377.17	3.46
120	374.89	2.27
140	375.69	1.54
160	376.06	1.13
180	375.21	0.82
200	378.62	0.62

The far-field simulation characteristics are summarized in Table 2. The symmetric broadbeam performance can be seen for all three principal planes. The desired 3-dB uniformity area of 80 mm × 80 mm, which corresponds to a symmetrical 2 × 2 deployment of four Petri dishes to suppress polarization effects [18], is fully accomplished over each vertical distance d as a result. Note that this 3-dB uniformity stems from the reasonable distributions of the PD over cultured cells for a practical experiment [13]. A high cross-polarization discrimination (XPD) of at least 20 dB is also obtained to ensure single polarization during exposures. The simulated wave impedance and uniformity results are listed in Table 3. Plane wave properties along shorter vertical distances and good uniformity performances are clearly seen. An amplifier output power is injected into this choke-ring type antenna for MMW uniformity inside the chamber. Note that an antenna is installed on the ceiling of the chamber for the direct MMW illumination into a cell layer for 3D culture experiments, as illustrated in Figure 3A.

An FLIR A325sc IR camera (FLIR Systems, Inc.) is also mounted on the ceiling of the chamber, as shown in Figure 3B, for temperature regulation during exposure. The measured camera temperatures are used as a target value for temperature regulation by adjusting the airflow cooling rate via real-time feedback to the incubator. It should be noted that most commercial incubators used for practical cell culture experiments do not contain an active air-cooling system [23,24] to prevent the temperature rise caused by MMW exposure [14,25].

A WR-28 waveguide probe (NSI-MI Technologies) placed at the bottom of the exposure chamber is used for uniformity measurements. An LTC5596 power detector (Analog Devices) is also connected at the output port of the chamber after a probe and measures the MMW signal power for the antenna input power control. An MA-60-05(10)-SS XY positioner (Hanguk Robot Ltd.) is mounted at the bottom of the chamber for horizontal probe positioning during the uniformity measurements. The vertical position of the probe can be manually adjusted by tightening or loosening a tuning screw. The practical uniformity inside the chamber for actual

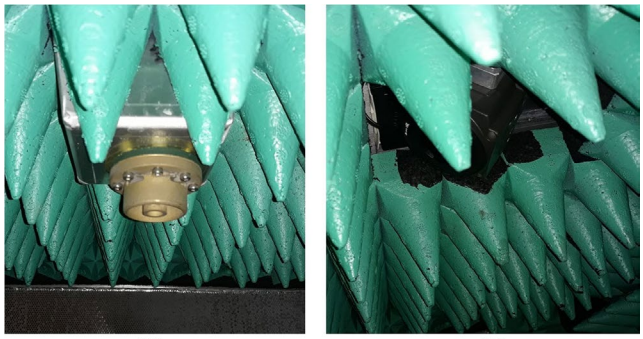

FIGURE 3 (A) Choke-ring type antenna and (B) IR camera installed on the ceiling of the exposure chamber

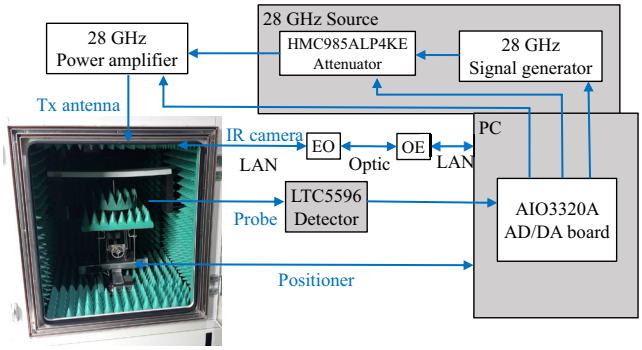

FIGURE 4 Schematic of the control flow of the in vitro 28 GHz exposure system

exposure over the target area is verified by the insertion loss (S_{21}) measurements along every vertical distance.

Finally, a KER-EPP10 MMW pyramidal absorber (Korea Electromagnetic Research) suitable for high humidity and temperature conditions is employed for all the internal walls of the exposure chamber. A holder tray is made of Rohacell foam (Evonik) with a dielectric constant (ε_r) of nearly one to suppress additional field disturbances. The holder tray can be positioned at different vertical heights with respect to the antenna aperture from 100 mm to 300 mm using height-control blocks of 20 mm thickness (that is, in 20 mm steps).

2.2.2 | Control software

The main control software (SW) was developed in C++ and installed on a personal computer (PC) to allow the quick and easy setup of an experimental condition. A graphical user interface (GUI) enables the easy setup and configuration of experimental conditions (input power, temperature, warning, and so on) before an exposure is started. All 28-GHz source controls (turning the signal on or off, changing the input power level, and so on) can be performed via the main SW GUI. The temperature averaged area for the IR camera (usually at the cell surface) can be defined as well. The signal power and temperature profiles are monitored and displayed in real-time, respectively. All measured data are stored at designated intervals in an American Standard Code for Information Interchange (ASCII) file format for further post-processing. A log history message enables the accurate diagnosis of system malfunctions.

Figure 4 shows the entire control flow of the in vitro 28-GHz exposure system. It can be observed that all controls are carried out and executed by the main SW installed on the PC. An AIO3320A AD/DA board (JS Automation Corp.) is mounted on the PC for the control signals of the 28-GHz source operations, that is, to turn on a signal generator and an amplifier with the specified sequence of the protection relay and to adjust the variable attenuator voltage for the antenna input power control.

3 | RESULTS AND DISCUSSION

3.1 | MMW uniformity characteristic

The antenna input power, that is, the amplifier output power injected into the antenna input port, was measured using an N9030B PXA spectrum analyzer (Keysight Technologies) with a 28WL + CK-40_CU waveguide directional coupler (A-INFO Inc.) as varying the attenuator voltage. A 28WHPL125 waveguide high-power load (A-INFO Inc.) was employed to terminate the waveguide coupler. Figure 5 shows the measurement result of an antenna input power in terms of the variable attenuator voltage. It can be observed that a maximum antenna input power of 10 W is ensured. Small local discontinuities in the overall smooth profile are due to the actual attenuation characteristic of a variable attenuator as the control voltage changes. These voltage values were extracted from the measurement data in Figure 5 to enable the antenna input power to be controlled through the SW GUI. In practice, the antenna input power control, in intervals of 0.1 W, was established in the main SW based on this procedure.

The uniformity was verified by S_{21} measurements between the choke-ring type antenna and waveguide probe inside the exposure chamber. An 8722ES vector network analyzer (VNA) (Keysight Technologies) was used for measurements and a full 2-port calibration was performed. The VNA was controlled at the PC through a general-purpose interface bus interface and synchronized with an XY positioner for automatic scanning and data acquisition. The actual S_{21} measurements were conducted on the exposure area over all possible vertical distances d from 120 mm to 300 mm at 20 mm intervals (that is, the interval of the holder tray positioning). A measurement at a distance of 100 mm cannot be carried out owing to the limits of the hardware, that is, the probe cannot be vertically positioned at such a short distance from the antenna aperture.

Figure 6 depicts the measured S_{21} distribution normalized with respect to the average value at a vertical distance d of 180 mm. It can be observed that a uniformity of approximately 3 dB (that is, the difference between the maximum and minimum values is 3 dB) is obtained along the x- and y-axes (E- and H-planes), respectively, over the target area of 80 mm × 80 mm (see also Figure 1). Note that the smaller values at the diagonal vertices rarely affect the practical exposure area occupied by circular Petri dishes during an experiment. This 3-dB uniformity can be reasonably compared with the previously reported in vitro exposure setup [13].

The most fundamental parameter of interest for in vitro MMW exposure should be PD, because safety limits in the international guidelines are specified in terms of the PD value at MMW frequencies [21,22]. Note that one of the essential requirements for an in vitro exposure system is the ability to provide exposure levels according to the safety limits so that potential electromagnetic field (EMF) health effects may be carefully studied [26]. Although various coupling effects should be considered to find a precise PD value at the planar near-field region, a reasonable approximation of the near-field PD can be found based on far-field concepts, especially for broadbeam antennas [27]. Hence, the PD of S inside the chamber can be written as [28]

$$S = \frac{P_{\mathrm{rec,p}}}{A_{\mathrm{e,p}}} = \frac{4\pi P_{\mathrm{rec,p}}}{\lambda^2 G_{\mathrm{p}}} = \frac{4\pi P_{\mathrm{in}} |S_{21}|^2}{\lambda^2 G_{\mathrm{p}}}, \quad (1)$$

where $P_{\mathrm{rec,p}} = P_{\mathrm{in}} |S_{21}|^2$ is the power received by the waveguide probe, P_{in} is the antenna input power, S_{21} is the measured insertion loss in the linear scale, $A_{\mathrm{e,p}} = \lambda^2 / G_{\mathrm{p}} 4\pi$ is the probe effective aperture, λ is the wavelength (at 28 GHz), and G_{p} is a probe gain of 6 dB, respectively. Table 4 lists the PD and uniformity results for every vertical distance d when the antenna input power P_{in} is 1 W. Note that these PD values are obtained when the probe is polarization matched and aligned with an antenna on the main axis [12,16]. The degradation of uniformity compared with the simulations in Table 3 is due to internal electromagnetic reflections caused by the different system components (probes, positioner, and so on), accuracy of the positioning system employed for the S_{21} measurements inside the exposure chamber, and the approximation used in (1) to determine the near-field PD. Nevertheless, it can be observed that a uniformity of approximately 3 dB is ensured over every vertical distance d. In addition, because the PD of 45.83 W/m^2 can be obtained at a distance of 100 mm based on polynomial extrapolation when the input power is 1 W, high-power exposures of up to 458.3 W/m^2 are realized using the maximum input power of 10 W, which is reasonably close to the desired value of 500 W/m^2 in Table 1. The effective uniformity required for in vitro MMW exposures can be much smaller than the target area of 80 mm × 80 mm considering an insert with a 10 mm diameter inside a Petri dish for a 3D cell culture (see also Figure 7).

3.2 | Temperature regulation

Four 35 mm Petri dishes with inserts for a 3D cell culture, as shown in Figure 7, were placed on the holder tray inside the exposure chamber to verify the temperature regulation during exposure. Saline solutions and Micropig Franz cell membranes (Medi Kinetics Co., Ltd.) were used as a practical model for the 3D cell culture experiments, which are usually composed of a culture medium and a reconstructed cell model [20]. The center-to-center distance between the dishes was 39 mm, in accordance with the exposure area [18]. Measurement areas were designated at all four cell surfaces in the inserts via the main SW. The IR camera recorded the cell temperatures (that is, the temperatures on the designated

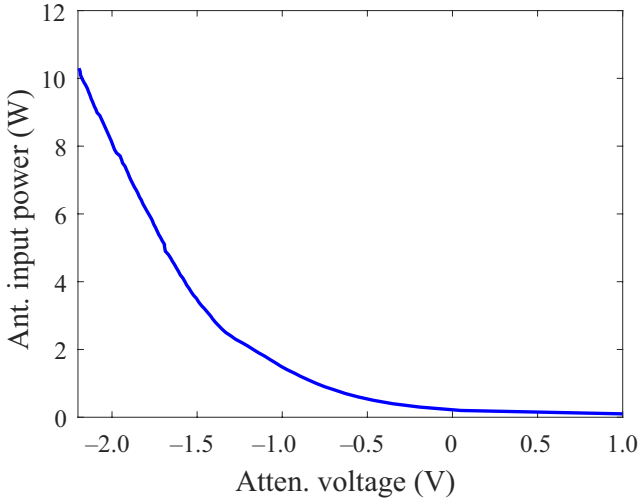

FIGURE 5 Measured antenna input power in terms of a variable attenuator voltage

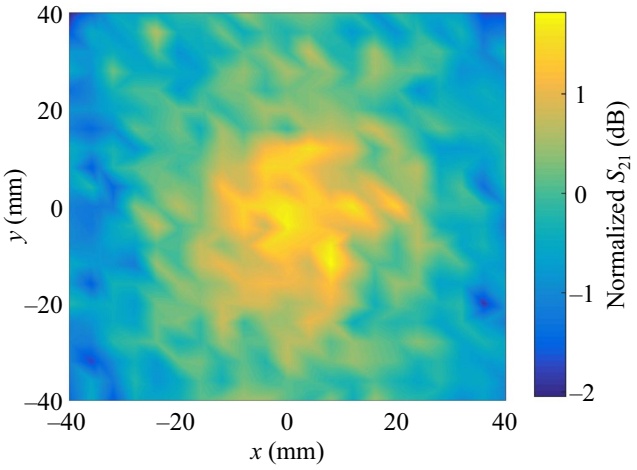

FIGURE 6 Normalized S_{21} distribution at a vertical distance d of 180 mm

areas) at 10 mseconds intervals, and the results were averaged for use as inputs to an incubator for air cooling (that is, real-time feedback). The target temperature for regulation was designated to be 37°C to provide an optimal thermal condition for cell cultures [13]. Note that the temperature cycle of the order of several hundred seconds is due to the time constant of a cooling system (that is, the required cooling time). The temperature profiles measured by the IR camera are presented in Figure 8 as a function of time at 160 mm when the antenna input power P_{in} is 0.5 W (that is, a PD of 10 W/m^2 equal to the safety limit [21,22]). Average cell temperatures maintained around the target value of 37°C despite the temperature rise caused by electromagnetic energy absorption due to MMW exposures [14,15]. The temperature profile across a 160-mm distance with a PD of approximately 200 W/m^2 is also shown in Figure 9. Despite a rapid rise in temperature owing to the high-power exposure, stable temperatures in the vicinity of 37°C can still be observed for a long period. Note that the temperature cycle that is shorter than that of the PD of 10 W/m^2 (Figure 8) is due to the larger amount of MMW absorption. These results indicate that reasonable temperature regulation can be accomplished based on the real-time feedback of the IR camera temperatures. It should be noted that this is an important feature of the implemented in vitro 28-GHz exposure system, in contrast to other reported MMW in vitro incubator setups [13,25], which are limited in use to low power exposures or require low incubation temperatures below 30°C to support high-power in vitro experiments due to cell temperature rises caused by MMW absorption. In contrast, the proposed system enables exposure experiments with various MMW PD levels because of its effective temperature regulation. Although the maintained average temperatures in Figures 8 and 9 are slightly higher than the optimal value of 37°C owing to the response delay time of the airflow cooling for system protection, this can be easily compensated for by adjusting the target temperature for the regulation, if required.

TABLE 4 PD and uniformity results for every vertical distance d (P_{in} is 1 W)

Vertical distance d (mm)	PD (W/m^2)	Uniformity (dB)
120	34.13	4.69
140	25.01	3.30
160	19.15	2.77
180	15.78	2.99
200	11.75	1.87
220	10.55	2.75
240	9.53	3.09
260	7.71	1.19
280	7.54	2.36
300	5.89	2.77

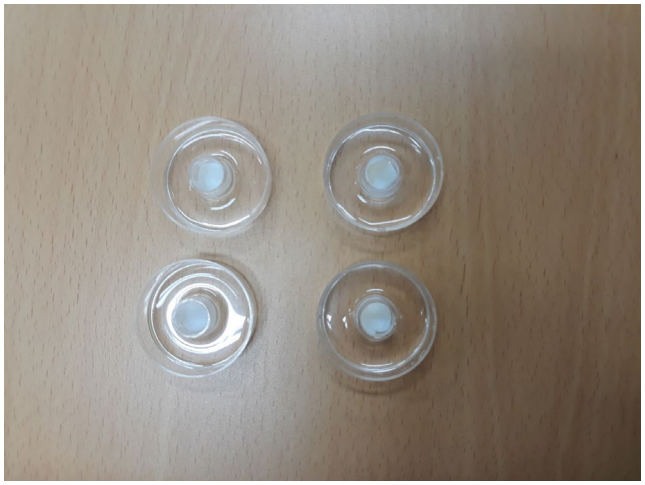

FIGURE 7 Four Petri dishes with inserts for 3D cell culture

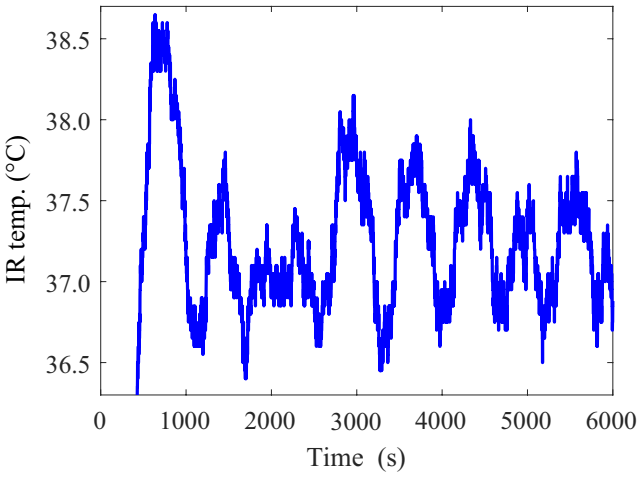

FIGURE 8 Temperature profile of the IR camera at a vertical distance d of 160 mm when antenna input power P_{in} is 0.5 W

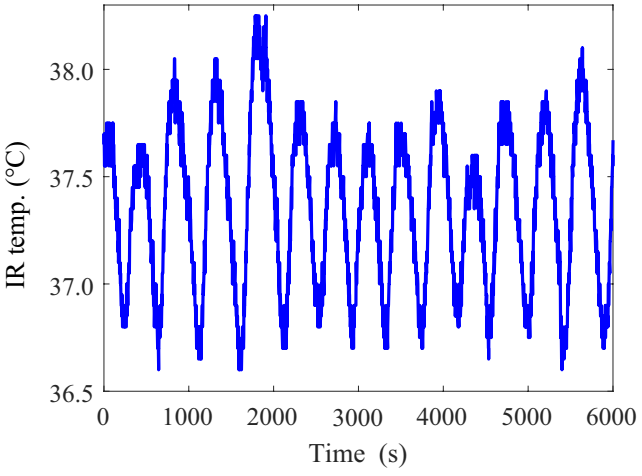

FIGURE 9 Temperature profile of the IR camera at a vertical distance d of 160 mm when antenna input power P_{in} is 10 W

4 | CONCLUSIONS

An in vitro 28-GHz exposure system based on field uniformity and a 3D cell culture was implemented. The 28-GHz signal source and power amplifier, customized for an exposure system, can produce a maximum output power of 10 W for high-power exposures. The antenna input power can be controlled using the measured value of the attenuator voltage and amplifier output power. The 3-dB uniformity generated by the designed choke-ring type antenna was verified by the S_{21} measurement over the target exposure area of 80 mm × 80 mm, which corresponds to four symmetrical Petri dishes to minimize the polarization effects for every vertical distance. The PD levels for practical in vitro experiments can also be controlled by adjusting the antenna input power as well as the vertical distance of the holder tray made of Rohacell foam with a ε_r of nearly one. The temperature regulation was verified using average cell temperatures measured by the IR camera. It was shown that the cell temperatures were successfully maintained in the vicinity of the optimal target value of 37°C under different 28-GHz exposure conditions (that is, at low and high PDs). This "all-in-one" exposure system enables more accurate and reliable in vitro 28-GHz experiments for investigating the potential health effects related to 5G MMW frequencies. Various in vitro 28-GHz experiments with high-power and long-term exposures will be carried out using the implemented in vitro integrated exposure system in future.

ACKNOWLEDGMENTS

The authors would like to thank Dymstec for their support and assistance during our system implementation. This work was supported by the ICT R&D program of MSIT/IITP. [2019-0-00102, A Study on Public Health and Safety in a Complex EMF Environment].

ORCID

Young Seung Lee https://orcid.org/0000-0002-7804-3241
Ae-Kyoung Lee https://orcid.org/0000-0002-8082-4194
Nam Kim https://orcid.org/0000-0001-8109-2055

REFERENCES

1. A. Ghosh et al., *5G evolution: A view on 5G cellular technology beyond 3GPP release 15*, IEEE Access **7** (2019), 127639–127651.
2. M. E. Leinonen et al., *28 GHz wireless backhaul transceiver characterization and radio link budget*, ETRI J. **40** (2018), no. 1, 89–100.
3. S. Henry, A. Alsohaily, and E. S. Sousa, *5G is real: evaluating the compliance of the 3GPP 5G new radio system with the ITU IMT-2020 requirements*, IEEE Access **8** (2020), no. 10, 42828–42840.
4. A. Aldalbahi, *Multi-backup beams for instantaneous link recovery in mmWave communications*, Electronics **8** (2019), no. 10, 1145.
5. T. Lv et al., *Millimeter-wave NOMA transmission in cellular M2M communications for internet of things*, IEEE Internet Things J. **5** (2018), no. 3, 1989–2000.
6. R. Ford et al., *Achieving ultra-low latency in 5G millimeter wave cellular networks*, IEEE Commun. Mag. **55** (2017), no. 3, 196–203.
7. *NR - Base station (BS) radio transmission and reception*, document TS 38.104, 3GPP, (2019), v. 15.8.0.
8. Y. S. Lee et al., *A study on the convenient EMF compliance assessment for base station installations at a millimeter wave frequency*, J. Electromagn. Eng. Sci. **18** (2018), no. 4, 242–247.
9. A. Perrin, and M. Souques, *Electromagnetic Fields*, Environment and Health, Springer-Verlag, France, 2012.
10. T. Wu, T. S. Rappaport, and C. M. Collins, *Safe for generations to come*, IEEE Microw. Mag. **16** (2015), no. 2, 65–84.
11. M. Simkó and M. Mattsson, *5G wireless communication and health effects – a pragmatic review based on available studies regarding 6 to 100 GHz*, Int. J. Environ. Res. Public Health **16** (2019), no. 18, 3406.
12. M. Zhadobov et al., *Evaluation of the potential biological effects of the 60-GHz millimeter waves upon human cells*, IEEE Trans. Antennas Propag. **57** (2009), no. 10, 2949–2956.
13. S. Koyama et al., *Long-term exposure to a 40-GHz electromagnetic field does not affect genotoxicity or heat shock protein expression in HCE-T or SRA01/04 cells*, J. Radiat. Res. **60** (2019), no. 4, 417–423.
14. M. Zhadobov et al., *Near-field dosimetry for in vitro exposure of human cells at 60 GHz*, Bioelectromagnetics **33** (2012), no. 1, 55–64.
15. J. X. Zhao, *Numerical dosimetry for cells under millimetre-wave irradiation using Petri dish exposure set-ups*, Phys. Med. Biol. **50** (2005), no. 14, 3405–3421.
16. J. Zhao and Z. Wei, *Numerical modeling and dosimetry of the 35 mm Petri dish under 46 GHz millimeter wave exposure*, Bioelectromagnetics **26** (2005), no. 6, 481–488.
17. T. S. Rappaport et al., *Millimeter wave mobile communications for 5G cellular: it will work!*, IEEE Access **1** (2013), 335–349.
18. Y. S. Lee et al., *Proposal of 28 GHz in vitro exposure system based on field uniformity for three-dimensional cell culture experiments*, Bioelectromagnetics **40** (2019), no. 7, 445–457.
19. K. Jung et al., *KeraSkin™-VM: a novel reconstructed human epidermis model for skin irritation tests*, Toxicol. in Vitro. **28** (2014), no. 5, 742–750.
20. W. Jang et al., *Evaluation of eye irritation potential of solid substance with new 3D reconstructed human cornea model, MCTT HCETM*, Biomol. Ther. **23** (2015), no. 4, 379–385.
21. ICNIRP, *Guidelines for limiting exposure to time-varying electric, magnetic, and electromagnetic fields (up to 300 GHz)*, Health Phys. **74** (1998), no. 4, 494–522.
22. ICNIRP, *Guidelines for limiting exposure to time-varying electric, magnetic, and electromagnetic fields (up to 300 GHz)*, Health Phys. **118** (2020), no. 5, 483–524.
23. J. Schuderer et al., *In vitro exposure apparatus for ELF magnetic fields*, Bioelectromagnetics **25** (2004), no. 8, 582–591.
24. N. Nikoloski et al., *Reevaluation and improved design of the TEM cell in vitro exposure unit for replication studies*, Bioelectromagnetics **26** (2005), no. 3, 215–224.
25. P. L. Pogam et al., *Untargeted metabolomics unveil alterations of biomembranes permeability in human HaCaT keratinocytes upon 60GHz millimeter-wave exposure*, Sci. Rep. **9** (2019), no. 1, 1–10.
26. F. Schönborn et al., *Basis for optimization of in vitro exposure apparatus for health hazard evaluations of mobile communications*, Bioelectromagnetics **22** (2001), no. 8, 547–559.
27. C. Newell, R. D. Ward, and E. J. Mcfarlane, *Gain and power parameter measurements using planar near-field techniques*, IEEE Trans. Antennas Propag. **36** (1988), no. 6, 792–803.

28. A. Balanis, *Antenna theory: analysis and design*, 3rd ed, John Wiley & Sons, New Jersey, 2005.

AUTHOR BIOGRAPHIES

Young Seung Lee received his MS and PhD degrees in electrical and electronic engineering from the Korea Advanced Institute of Science and Technology, Daejeon, Rep. of Korea, in 2008 and 2012, respectively. Since 2012, he has been with the Electronics and Telecommunications Research Institute, Daejeon, Rep. of Korea, where he is presently a senior researcher. His current research interests are in the fields of exposure system design, compliance assessment, and numerical dosimetry with an emphasis on 5G and millimeter-wave frequencies. He is also concerned with electromagnetic theory and antenna propagation.

Philip Ayiku Dzagbletey received his BSc in telecommunication engineering from KNUST, Kumasi, Ghana in 2013 and MSc from Hanbat University, Daejeon, Rep. of Korea, in 2016. He received his PhD in electrical engineering at Seoul National University of Science and Technology, Seoul, Rep. of Korea, and was the best paper recipient at an IEEE-KIEES conference. Much of his research interests have been in microwave and millimeter-wave antenna and circuit design for industrial and commercial use. He has completed several projects, including 5G antenna measurement systems, millimeter-wave antenna array systems, and wearable fabric antennas.

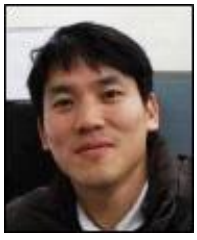

Jae-Young Chung received his BS degree from Yonsei University, Seoul, Rep. of Korea, in 2002, and his MS and PhD degrees from the Ohio State University, USA, in 2007 and 2010, respectively; all degrees were in electrical engineering. From 2002 to 2004, he was with Motorola as an RF engineer. From 2010 to 2012, he worked at Samsung Electronics, Suwon, Rep. of Korea, as an antenna engineer. He is currently an associate professor with the Department of Electrical and Information Engineering, Seoul National University of Science and Technology, Seoul, Rep. of Korea. His research interests include electromagnetic measurement and antenna design.

Sang Bong Jeon received his BS, MS, and PhD degrees in electronic engineering from Yeungnam University, Gyeongsan, Rep. of Korea, in 2001, 2003, and 2007, respectively. From 2008 to 2010, he was a senior research engineer at the Korea Radio Promotion Association, Seoul, Rep. of Korea, where he conducted research in the fields of electromagnetic compatibility technology. Since 2010, he has been with Radio & Satellite Research Division, Electronics and Telecommunications Research Institute, Daejeon, Rep. of Korea. His research interests include bioelectromagnetics and electromagnetic compatibility.

Ae-Kyoung Lee received her BS and MS degrees in electronics and engineering from Chungang University, Seoul, Rep. of Korea, in 1990 and 1992, respectively, and her Ph.D. in radio science and engineering from Chungnam National University, Daejeon, Rep. of Korea, in 2003. In 1992, she joined the Radio Technology Group at the Electronics and Telecommunications Research Institute, Daejeon, Rep. of Korea, where she has been involved in projects on measurement technologies and numerical analyses of electromagnetic compatibility and human exposure to RF fields. Dr. Lee was the recipient of the Japan Microwave Prize at the 1998 Asia-Pacific Microwave Conference, Japan, and the Technology Award from the Korea Electromagnetic Engineering Society in 1999.

Nam Kim received his BS, MS, and PhD degrees in electronics engineering from Yonsei University, Seoul, Rep. of Korea, in 1981, 1983, and 1988, respectively. Dr. Kim is a member of the International Advisory Committee for the World Health Organization project on EMF, the IEEE International Committee on Electromagnetic Safety, and the International Electrotechnical Commission TC 106, and he was the president of the Bioelectromagnetics Society. He has been a professor in the School of Information and Communication Engineering, Chungbuk National University, Chengju, Rep. of Korea, since 1989. His scientific interests are focused on optical information processing, the health effect of EMF, wireless power transfer, and antennas for mobile communications.

Seong Jong Song has completed his bachelor's degree in economics from the University of California at San Diego, USA, in 2011. He has been working at Dymstec, Seongnam, Rep. of Korea, for eight years. He is responsible for leading, developing, and managing company tactical operations.

Hyung-Do Choi received his MS and PhD degrees in material sciences from Korea University, Seoul, Rep. of Korea, in 1989 and 1996, respectively. Since 1997, he has been with the Electronics and Telecommunications Research Institute, Daejeon, Rep. of Korea, where he is presently a project leader of the Radio & Satellite Research Division. He researched in the field of biological effects of RF radiation and developed RF radiation protection standards.